Imaging of Uterine Carcinoma by Carbon-11-Methionine and PET

Maria Lapela, Sirkku Leskinen-Kallio, Matti Varpula, Seija Grenman, Kalle Alanen, Kjell Någren, Pertti Lehikoinen, Ulla Ruotsalainen, Mika Teräs and Heikki Joensuu

Department of Oncology and Radiotherapy, Department of Pathology, and Turku Medical Cyclotron/PET Center, Turku University; Medical Imaging Center and Department of Obstetrics and Gynecology, Turku University Central Hospital, Turku, Finland

L-[methyl-^{11}C]methionine ([^{11}C]methionine) is probably one of the most useful positron-emitting tracers for metabolic imaging of human cancer. In this study, we investigated whether human uterine cancer can be imaged with [^{11}C]methionine and PET. **Methods:** Fourteen patients with primary uterine malignancy participated in the study. Eight patients had endometrial carcinoma and six had cervical carcinoma. The normal endometrium was analyzed in four additional patients with no uterine malignancy and in one patient with cervical cancer. Tracer uptake was quantitated by calculating both the standardized uptake values (SUVs) and the kinetic influx constants (K_i values) for the tracer. **Results:** All patients with either cervical or endometrial carcinoma had increased uptake of [^{11}C]methionine in the PET image. The mean SUV of the carcinomas was 8.4 (n = 13; s.d., 1.5) and the mean K_i was 0.15 min^{-1} (n = 12; s.d., 0.08 min^{-1}), whereas the mean SUV of the normal endometrium was only 4.6 (n = 5; s.d., 0.8). Histologically poorly (Grade III) or moderately (Grade II) differentiated endometrial carcinomas accumulated more [^{11}C]methionine than the well-differentiated (Grade I) ones ($p = 0.04$ for the SUVs, and $p = 0.05$ for the K_i values). There were also variable physiological accumulations of [^{11}C]methionine in the pelvis. **Conclusions:** Uterine carcinoma accumulated [^{11}C]methionine more than the normal endometrium. However, the physiological accumulations of [^{11}C]methionine in the pelvis may confuse the interpreter of the PET image; thus, morphological imaging also needs to be performed as a reference to localize the tumor accurately. We conclude that human uterine carcinoma can be effectively imaged with [^{11}C]methionine and PET.

Key Words: PET; methionine; uterine cancer

J Nucl Med 1994; 35:1618–1623

Computed tomography (CT) and magnetic resonance imaging (MRI) are widely used to image uterine cancer, whereas metabolic imaging of gynecologic cancer is still in its infancy. Uptake of [^{18}F]fluorodeoxyglucose in human ovarian cancer (*1,2*) and in cancer of the fallopian tubes (*3*) has been reported, but there are currently no human studies reported on accumulation of [^{11}C]methionine in gynecologic cancer in the literature.

Methionine is an essential amino acid needed for protein and polyamine synthesis and in transmethylation reactions, and its metabolism is accelerated in malignant cells (*4*). The increased utilization of this amino acid can be measured by PET with radiolabeled L-[methyl-^{11}C]methionine ([^{11}C]methionine) used as the tracer.

Carbon-11-methionine has been successfully used for metabolic imaging of brain (*5*) and lung (*6*) tumors, non-Hodgkin's lymphoma (*7*), breast cancer (*8*) and head and neck cancer (*9*). The uptake of [^{11}C]methionine appears to correlate with the histological grade of brain (*10*) and lung tumors (*11*), whereas an association between the grade of differentiation of cancer and high [^{11}C]methionine uptake could not be verified in small series of patients with head and neck cancer (*9*) or lymphoma (*7*).

The aim of the present study was to investigate whether human cervical and endometrial cancer can be imaged with [^{11}C]methionine and PET, and to study the association between the uptake of [^{11}C]methionine and histological grade of uterine cancer.

PATIENTS AND METHODS

Patients

Fourteen patients with uterine malignancy who were admitted to the Department of Gynecology and Obstetrics, Turku University Central Hospital between November 1992 and September 1993 participated in the study. Patient and carcinoma characteristics are presented in Table 1. Eight patients had endometrial carcinoma, seven of which were adenocarcinomas and one adenosquamous cell carcinoma. Six patients had squamous-cell carcinoma of the uterine cervix. Staging of the tumors was done according to the International Federation of Gynecology and Obstetrics (FIGO) (*12*). Clinical staging was used for cervical cancer, and surgical staging for endometrial cancer except for Patient 14 who did not undergo surgery. Tumor size was measured from the CT or MR images. The body mass index (BMI) (*13*) was calculated as weight (kg) divided by the square of height (m^2); it varied from 20.0 to 36.6 kg/m^2 (median, 24.0 kg/m^2).

Accumulation of [^{11}C]methionine in the normal endometrium was analyzed in four other women aged 35, 41, 48 and 50, who

Received Dec. 28 1993; revision accepted Mar. 23, 1994.

For correspondence or reprints contact: Maria Lapela, MD, Department of Oncology and Radiotherapy, Turku University Central Hospital, FIN - 20 520 Turku, Finland.

TABLE 1
Patient and Tumor Characteristics

Patient no.	Age	Location	Histology	Stage (FIGO)	Histological grade
1	33	Cervix	scc	IB	II
2	83	Cervix	scc	IIA	III
3	74	Cervix	scc	IIB	II
4	78	Cervix	scc	IIB	III
5	73	Cervix	scc	IIIB	II
6	35	Cervix	scc	IIIB	II
7	52	Endometrium	ac	IA	I
8	68	Endometrium	ac	IA	I
9	55	Endometrium	ac	IB	I
10	67	Endometrium	ac	IB	I
11	56	Endometrium	ac	IB	II
12	48	Endometrium	asc	IIIC	III
13	76	Endometrium	ac	IVA	III
14	73	Endometrium	ac	IVB	II

scc = squamous-cell carcinoma, ac = adenocarcinoma, asc = adenosquamous-cell carcinoma.
Histologically well (Gr. I), moderately (Gr. II) or poorly (Gr. III) differentiated.

underwent PET imaging for ovarian tumors (n = 2) or osseous metastases from breast cancer located in the pelvis (n = 2). In two of these patients, the uterus was found to be macroscopically normal at laparotomy; it was also normal after histological examination. For all patients the uterus was normal on the CT images. In addition, uptake in the normal endometrium was analyzed in Patient 1 (Table 1), who had surgery for cervical cancer, and the endometrium was found to be benign in histopathological examination.

All PET studies were performed prior to any treatment for uterine cancer except for Patient 5 (Table 1), who had received radiotherapy for four days (the total cumulative dose of 8 Gy) prior to the PET study. All patients fasted for more than 4 hr before the PET study except Patient 3 (Table 1) who had fasted for 2 hr.

Written informed consent was obtained from all patients and the study was approved by the Ethical Committee of Turku University Central Hospital.

Histology

Histological verification was based on analysis of samples taken at surgery (*14,15*). If surgery was not performed (Patients 2, 4, 5, 6, and 14, Table 1), histological evaluation was based on the specimens taken by fractionated curettage and/or biopsy. Histological grading was done without any knowledge of the PET data.

CT and MR Imaging

For accurate localization of the tumors, the endometrial cavity and the uterine cervix, CT (General Electric CT Pace scanner) and/or MRI (Siemens Magnetom 1.5 T superconducting unit) were performed in all patients. In CT examinations, the slice thickness was 5 mm or 10 mm. Intravenous contrast enhancement was used in every case. T2-weighted axial and sagittal images were obtained in MR examinations. Slice thickness was 5 mm or 8 mm. No intravenous contrast enhancement was used. The CT and the MR scans were interpreted by a radiologist with special interest in radiology of the female genital organs, and who was aware of the PET study results and the surgical and histological findings.

PET Imaging

Carbon-11-methionine was synthesized at the Radiopharmaceutical Chemistry Laboratory of Turku University Cyclotron/PET Center as described by Långström et al. (*16*) with slight modifications. The radiochemical purity of the tracer was measured as described elsewhere (*17*) and varied from 93.3% to 98.1% (mean, 96.0%). The impurities were [^{11}C]methionine sulfoxide and D-[^{11}C]methionine, which were present in about equal amounts.

An ECAT 931/08-12 PET scanner (Siemens/CTI Corp., Knoxville, TN) was used for PET imaging. The device acquires 15 contiguous slices simultaneously with a slice thickness of 6.7 mm; the transaxial FWHM in the center of the field of view measured according to Spinks et al. is 6.1 mm (*18*).

To correct for photon attenuation, a transmission scan was obtained prior to emission imaging with a removable ring source containing ^{68}Ge (total collected counts over 15×10^6 per plane). A bolus of [^{11}C]methionine (mean, 290 MBq; range, 200–350 MBq) was injected into a peripheral vein of the upper extremity, and dynamic emission acquisition followed for 40 min (4 × 30 sec, 3 × 60 sec, 5 × 180 sec, and 4 × 300 sec). All data were corrected for deadtime, decay and photon attenuation and were reconstructed in a 256 × 256 matrix with a Hann filter (cut-off frequency 0.5).

For Patient 6, imaging was performed for 34 min. Patient 5 was investigated from 36 to 51 min after injection with three frames, and was excluded from the kinetic analysis. The accumulation of tracer in Patient 4 could not be quantitated for logistical reasons and was only included in the qualitative analysis (Table 2).

Radioactivity in plasma was measured from 16 to 21 blood samples taken from an antecubital vein contralateral to the injection site. The low molecular weight fraction of plasma taken at 20–25, 40 and 60 min after injection was separated by fast gel filtration (Sephadex PD-10 columns, Pharmacia Fine Chemicals, Sweden) for radioactivity measurements (*19*).

ROI Analysis

Dynamic images were summed together over a period from 5 to 40 min, and localization in the tissues of interest was confirmed

TABLE 2
Cancer Detection

Patient no.	Tumor size (mm)	Endometrium (mm)*	CT	MRI	SUV	K_i
1	15 × 10 × 30	—	no	yes	8.8	0.15
2	15 × 15 × 15	—	yes	yes	8.0	0.17
3	25 × 25 × 25	—	yes	yes	8.8	0.11
4	50 × 35 × 40	—	yes	yes	n.d.	n.d.
5	50 × 50 × 60	—	yes	n.d.	8.3	n.d.
6	60 × 50 × 60	—	yes	n.d.	11.2	0.28
7	n.d.	7	no	n.d.	6.4	0.09
8	n.d.	8	no	n.d.	8.6	0.09
9	n.d.	1	n.d.	no	5.6	0.10
10	15 × 20 × 20	3	yes	n.d.	7.3	0.10
11	n.d.	5	no	no	7.3	0.12
12	n.d.	25	no	n.d.	8.3	0.10
13	10 × 80 × 50	>20	yes	n.d.	10.5	0.22
14	50 × 60 × 50	n.d.	yes	yes	9.8	0.31

*Thickness of malignant endometrium determined by microscopy. n.d. = not determined; SUV = standardized uptake value; K_i = influx constant.

using CT or MR images. Regions of interest (ROIs) were drawn on the hot spots of the tumor and on the normal tissues in the last frame of the dynamic imaging. The ROIs in normal tissues were drawn in the acetabulum, the iliac, the sacral and the pubic bones, and in the intestinal area, if they were clearly visible and reliably identifiable on the summed image.

Tracer accumulation in the ROIs was measured using the standardized uptake value (SUV), which is the radioactivity concentration in a ROI divided by the injected dose and the patient's weight (*20*). The ROIs with the maximum average counts were selected to represent [^{11}C]methionine uptake in the tissues.

A graphical approach according to Patlak et al. (*21*) was used to calculate the [^{11}C]methionine uptake rate from the plasma into the tissue as influx constants (K_i values). The radioactivity concentration of the low molecular weight fraction of plasma was used as the input function. The last eight data points representing the time from 8 to 40 min after the tracer injection were used to produce the influx curve.

Statistical Analysis

Student's t-test was used to compare the SUVs and K_i values between different groups. SUVs and K_i values were compared with linear regression. All p values are two-sided.

RESULTS

All 14 carcinomas accumulated [^{11}C]methionine in the PET imaging, although the intensity of the uptake varied (Table 2, Figs. 1 and 2). In comparison, CT was performed in 13 patients, and cancer was detectable in only eight patients. MRI was done on seven patients, and cancer could be detected in five (Table 2). The cervical tumor of Patient 1 could not be discerned from the surrounding normal cervical tissue in a CT scan although intravenous contrast enhancement was used. In T2-weighted MR images, the tumor was well delineated. In Patients 7, 8, 9, 11 and 12, the uterus could not be interpreted as abnormal either on CT or MRI. The endometrial cavities were not dilated, and the tumors were not large enough to be detected by CT or MRI.

The SUVs of the carcinomas varied from 5.6 to 11.2 (n = 13; mean ± s.d., 8.4 ± 1.5), and the K_i values from 0.09 min^{-1} to 0.31 min^{-1} (n = 12; 0.15 ± 0.08 min^{-1}, Table 2). The K_i values and the SUVs measured for the same tumor correlated well with each other (n = 12; r = 0.78; p = 0.003). The mean SUV of cervical squamous-cell carcinomas was 9.0 (n = 5; s.d., 1.2), and that of endometrial carcinomas 8.0 (n = 8; s.d., 1.7; p = 0.12, Fig. 3).

For Patient 14, two pelvic and one vaginal metastases visible in a CT and a MRI scan could be studied in addition to the primary tumor (Fig. 3). The SUVs of the metastases (7.7, 9.6 and 10.1) were similar to that measured from the primary tumor (9.8). Two other patients had small lymph node metastases in histological specimens that were be-

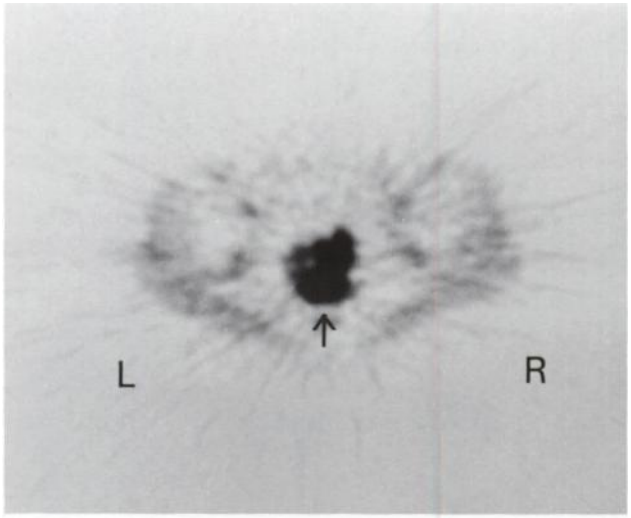

FIGURE 1. Carbon-11-methionine PET image of a patient with cervical squamocellular carcinoma that caused hydronephrosis (Stage IIIB, arrow; Patient 6, Tables 1 and 2). The SUV of the tumor is 11.2, and the K_i value is 0.28.

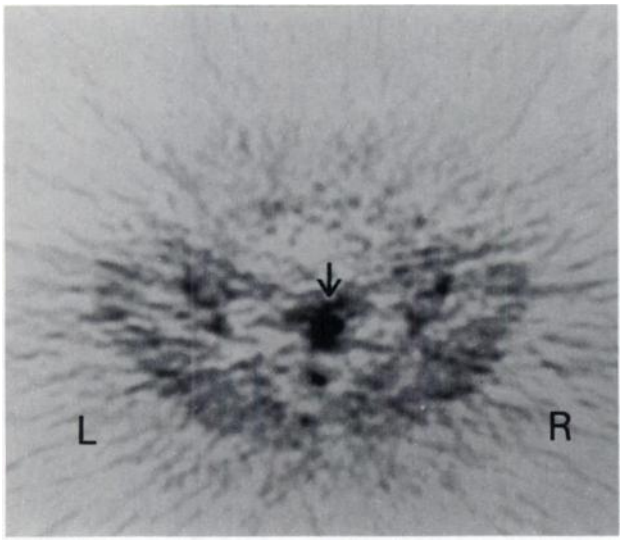

FIGURE 2. Carbon-11-methionine PET image of a patient with endometrial adenocarcinoma (arrow) Stage IA (Patient 8, Tables 1 and 2). The SUV of the tumor is 8.6, and the K_i value is 0.09. The small hot spot posterior to the uterine lesion is the bowel.

yond the resolution limit of the PET device, and they were not visible on CT/MR scans either.

The uptake of [^{11}C]methionine was generally higher in the malignant lesions than in the normal tissues (Fig. 3). The mean SUV of the acetabulum was 4.4 (n = 11; s.d., 0.7), the iliac bone 5.3 (n = 11; s.d., 1.2), the sacral bone 5.8 (n = 5; s.d., 1.3), the pubic bone 4.6 (n = 6; s.d., 1.3), and the bowel 5.6 (n = 10; s.d., 0.95). The bladder was visible in three patients with SUVs of 5.6, 6.6 and 16.1.

The mean SUV of the normal endometrium was 4.6 (n = 5; s.d., 0.79, Fig. 3). Four of these patients were premenopausal; two had the secretorial phase of the menstrual cycle with a SUV of 5.5 and 5.2, and two others had the proliferative phase with a SUV of 4.6 and 4.2. The remaining patient was postmenopausal with a SUV of 3.5. The difference between the SUVs of the normal endometrium and those of endometrial carcinomas was statistically significant (p = 0.0007).

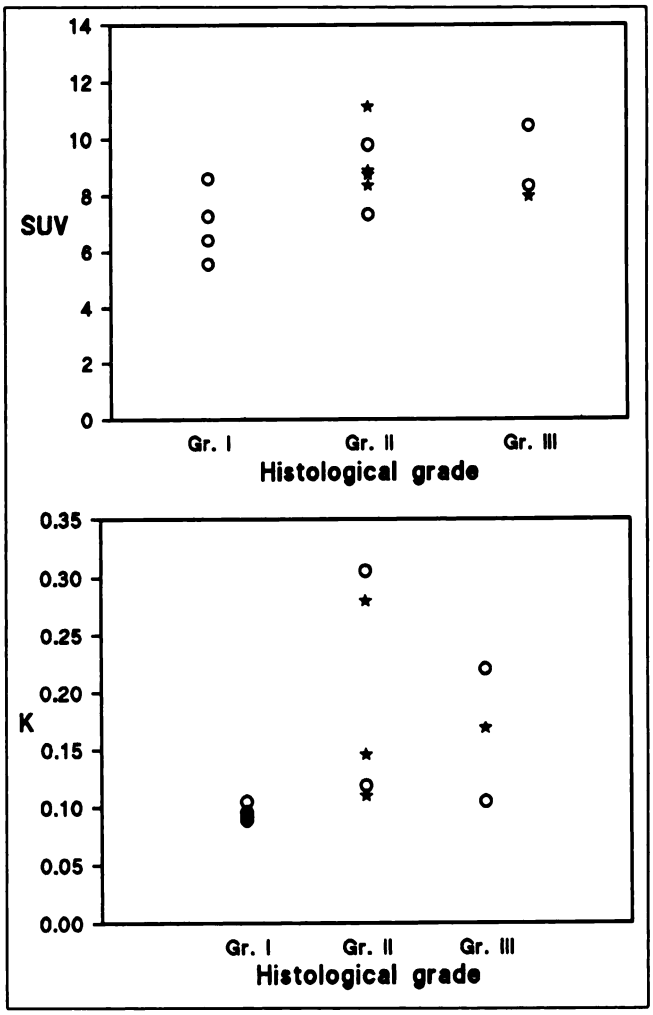

FIGURE 4. (A) Association between histological grade and the SUV. (B) Association between histological grade and the K_i value. Grades I, II and III: well, moderately, and poorly differentiated carcinoma, respectively. Star = cervical carcinoma, circle = endometrial carcinoma.

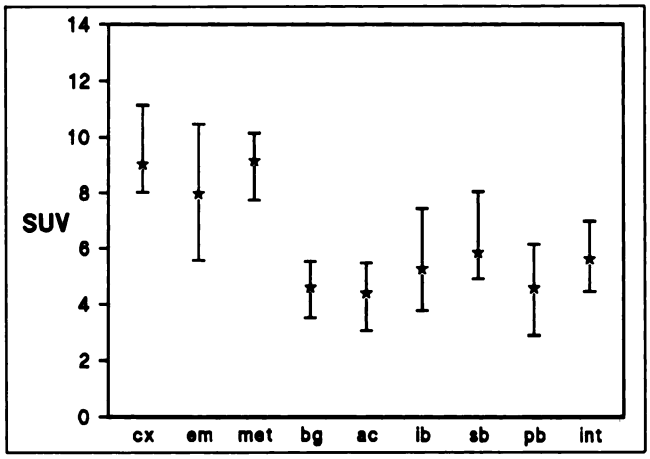

FIGURE 3. The SUVs of malignant and some normal tissues (mean and range). cx = cervical cancer (n = 5), em = endometrial cancer (n = 8), met = metastasis of endometrial cancer (n = 3), bg = benign (normal) endometrium (n = 5), ac = the acetabulum (n = 11), ib = the iliac bone (n = 11), sb = the sacral bone (n = 5), pb = the pubic bone (n = 6), int = the intestinal area (n = 10).

The SUVs and the K_i values of the tumors plotted against the histological grade are shown in Figure 4, and the SUVs against the FIGO stage in Figure 5. Poorly (Grade III) or moderately (Grade II) differentiated carcinomas accumulated more [^{11}C]methionine than the well-differentiated (Grade I) ones (p = 0.01 for the SUVs, and 0.03 for the K_i values). Similarly, in the subset of patients with endometrial carcinoma (n = 8), the SUVs and the K_i values were higher in poorly or moderately differentiated cancers than in well differentiated ones (p = 0.04 and 0.05, respectively).

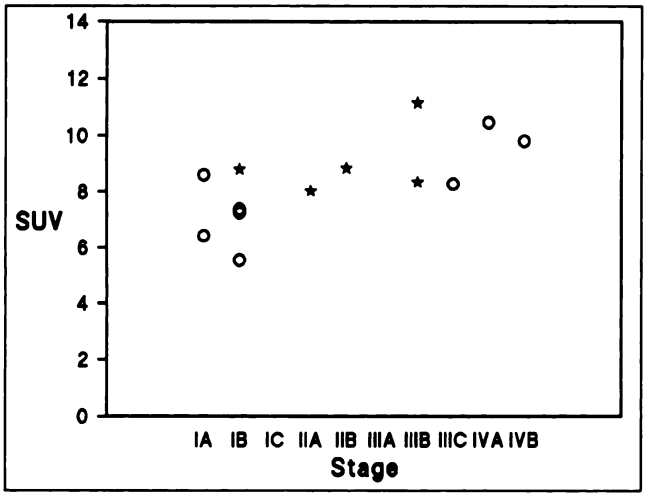

FIGURE 5. The SUV of cervical (star) and endometrial (circle) carcinomas by the FIGO stage.

DISCUSSION

All 14 uterine carcinomas were detectable in the [^{11}C]methionine image. The CT and the MRI findings were interpreted by an experienced radiologist who was aware of the clinical and PET data, however, all carcinomas were not visible on the CT or MR scans (Table 2). Although PET imaging with [^{11}C]methionine is sensitive for detecting malignant changes in the uterus, it cannot replace CT or MRI as a diagnostic tool at its present stage of development. CT or MRI is needed to visualize the normal structures of the pelvis and to ensure accurate localization of the hot spots found in the PET image. Especially in the cases where the tumor has low tracer uptake, the physiological accumulations of [^{11}C]methionine may interfere with the PET analysis unless other imaging studies are performed. Although the bladder was in the field of view, only three patients had clear accumulation of activity in the bladder. The reason for this variable accumulation is currently not known. However, the activity in the bladder did not hinder analysis of the nearby tissues in the present study, but it could be a source of error if bladder tumors had been studied.

Uptake of [^{11}C]methionine was lower in the normal endometrium than in endometrial cancer. However, the effect of the menstrual cycle on the uptake of [^{11}C]methionine is still unknown. Also, in patients with endometrial cancer, hormonal status may contribute to methionine uptake values. The relatively high uptake of methionine in the normal endometrium may lower the specificity of [^{11}C]methionine PET to distinguish especially small, low-grade malignant lesions from the normal uterus.

Patient 7 had atypical adenomatous hyperplasia with focal adenocarcinoma present in the endometrium, and patient 9 had only a 1-mm layer of invasive endometrial adenocarcinoma that was histologically found in the myometrium. The SUVs of these patients were the lowest measured in this series (6.4 and 5.6, respectively) and approached the values found in the secretory phase of the normal endometrium in premenopausal women. The partial volume effect lowers the measured tracer uptake values of these small carcinomas. On the other hand, uptake of methionine in reactive normal cells may also have contributed to the increased accumulation of [^{11}C]methionine in these patients.

An association between poor differentiation grade of carcinoma and high uptake of [^{11}C]methionine was found. Such an association was found when only patients with endometrial cancer were analyzed, and also when all patients with either adenocarcinoma or squamous-cell carcinoma were included in the same analysis. The association between poor histological grade of differentiation and high uptake of [^{11}C]methionine is in line with earlier studies, in which high [^{11}C]methionine uptake has been found in carcinomas of the breast and the lung with a high cell proliferation rate (*8,22*). However, the result needs to be confirmed in a larger series of patients.

In conclusion, [^{11}C]methionine and PET is an effective method for imaging uterine cancer, although physiological uptake of [^{11}C]methionine in the bone marrow and bowel also occurs. Further studies are needed to evaluate how accurately [^{11}C]methionine PET can differentiate malignant lesions from benign tumors of the uterus, and to study how the menstrual cycle influences [^{11}C]methionine uptake. According to this study, PET with [^{11}C]methionine may be more sensitive than CT or MRI in detecting uterine cancer.

ACKNOWLEDGMENTS

The authors thank Professors Eeva Nordman and Uno Wegelius, and Tuula Salmi, MD, for valuable support. They also thank the personnel of the Imaging Center and the Department of Gynecology and Obstetrics for cooperation. Financial support provided by the Finnish Cancer Society and the Turku University Foundation.

REFERENCES

1. Hubner KF, McDonald TW, Smith GT, Gould HR, Buonocore E. Dynamic F-18-FDG studies for assessing ovarian cancer [Abstract]. *J Nucl Med* 1993;34:6P.
2. Gupta N, Muths C, Casey M, Frank A, Terry J, Chandramouli B. Detection of residual/recurrent ovarian cancer using PET-FDG imaging [Abstract]. *J Nucl Med* 1993;34:7P.
3. Karlan BY, Hoh C, Tse N, Futoran R, Hawkins R, Glaspy J. Whole-body positron emission tomography with (fluorine-18)-2-deoxyglucose can detect metastatic carcinoma of the fallopian tube. *Gynecol Oncol* 1993;49:383–388.
4. Hoffman RM. Unbalanced transmethylation and the pertubation of the differentiated state leading to cancer. *Bio Essays* 1990;12:163–166.
5. Ericson K, Lilja A, Bergström M, et al. Positron emission tomography with ([^{11}C]methyl)-L-methionine, [^{11}C]-D-glucose, and [^{68}Ga]EDTA in supratentorial tumors. *J Comput Assist Tomogr* 1985;9:683–689.
6. Kubota K, Matsukawa T, Ito M, et al. Lung tumor imaging by positron emission tomography using C-11 L-methionine. *J Nucl Med* 1985;26:37–42.
7. Leskinen-Kallio S, Ruotsalainen U, Någren K, Teräs M, Joensuu H. Uptake of carbon-11-methionine and fluorodeoxyglucose in non-Hodgkin's lymphoma: a PET study. *J Nucl Med* 1991;32:1211–1218.
8. Leskinen-Kallio S, Någren K, Lehikoinen P, Ruotsalainen U, Joensuu H. Uptake of [^{11}C]methionine in breast cancer studied by PET. *Br J Cancer* 1991;64:1121–1124.
9. Leskinen-Kallio S, Någren K, Lehikoinen P, Ruotsalainen U, Teräs M, Joensuu H. Carbon-11-methionine and PET is an effective method to image head and neck cancer. *J Nucl Med* 1992;33:691–695.

10. Derlon JM, Bourdet C, Bustany P, et al. [^{11}C]L-methionine uptake in gliomas. *Neurosurgery* 1989;25:720–728.
11. Fujiwara T, Matsukawa T, Kubota K, et al. Relationship between histologic type of primary lung cancer and carbon-11-L-methionine uptake with positron emission tomography. *J Nucl Med* 1989;30:33–37.
12. Revised FIGO staging for gynaecological cancer. *Br J Obstet Gynecol* 1989;96:889–892.
13. Olefsky JM. Obesity. In: Wilson JD, Braunwald E, Isselbacher KJ, et al. *Harrisons's principles of internal medicine, volume 1*, 12th ed. New York: McGraw-Hill; 1991:411.
14. Ferenczy A. Carcinoma and other malignant tumors of the cervix. In: Blaustein A, ed. *Pathology of the female genital tract*, 2nd ed. New York-Berlin-Heidelberg-Tokyo: Springer-Verlag; 1984:184–222.
15. Kurman RJ, Norris HJ. Endometrial neoplasia: hyperplasia and carcinoma. In: Blaustein A, ed. *Pathology of the female genital tract*, 2nd ed. New York-Berlin-Heidelberg-Tokyo: Springer-Verlag; 1984:311–351.
16. Långström B, Antoni G, Gullberg P, et al. Synthesis of L- and D-[methyl-^{11}C]methionine. *J Nucl Med* 1987;28:1037–1040.
17. Någren K. Quality control aspects in the preparation of [^{11}C]methionine. In: Mazoyer BM, Heiss WD, Comar D, eds. *PET studies on amino acid metabolism and protein synthesis*. Dordrecht: Kluwer Academic Publishers; 1993:81–87.
18. Spinks TJ, Jones T, Gilardi MC, Heather JD. Physical performance of the latest generation of commercial positron scanner. *IEEE Trans Nucl Sci* 1988;35:721–725.
19. Lundqvist H, Stålnacke C-G, Långström B, Jones B. Labelled metabolites in plasma after i.v. administration of [^{11}CH3]-L-methionine. In: Greits T, Widen L, Ingvar D, eds. *The metabolism of the human brain studied with positron emission tomography*. New York: Raven Press; 1985:233–240.
20. Woodard HW, Bigler RB, Freed B, Russ G. Expression of tissue isotope distribution. *J Nucl Med* 1975;16:958–959.
21. Patlak CS, Blasberg RG, Fenstermacher JD. Graphical evaluation of blood-to-brain transfer constants from multiple-time uptake data. *J Cerebr Blood Flow Metab* 1983;3:1–7.
22. Miyazawa H, Arai T, Iio M, Hara T. PET imaging of non-small-cell lung carcinoma with carbon-11-methionine: relationship between radioactivity uptake and flow cytometric parameters. *J Nucl Med* 1993;34:1886–1891.